Available online at www.sciencedirect.com
ScienceDirect
Intermetallics 16 (2008) 225–229
Intermetallics
www.elsevier.com/locate/intermet

Enhancement of corrosion resistance in bulk metallic glass by ion implantation

Q.K. Jiang [a], C.L. Qin [b,**], K. Amiya [c], S. Nagata [c], A. Inoue [c], R.T. Zheng [d], G.A. Cheng [d], X.P. Nie [a], J.Z. Jiang [a,*]

[a] International Center for New-Structured Materials (ICNSM), Zhejiang University and Laboratory of New-Structured Materials, Department of Materials Science and Engineering, Zhejiang University, Hangzhou 310027, PR China
[b] Japan Science and Technology Agency, Institute for Materials Research, Tohoku University, 2-1-1 Katahira, Aoba-ku, Sendai, Japan
[c] Institute for Materials Research, Tohoku University, 2-1-1 Katahira, Aoba-ku, Sendai, Japan
[d] Key Laboratory of Beam Technology and Material Modification of Ministry of Education, Department of Materials Science and Engineering, Beijing Normal University, Beijing 100875, PR China

Received 10 July 2007; received in revised form 26 September 2007; accepted 28 September 2007
Available online 7 November 2007

Abstract

In this paper, ion-implantation technique was applied to improve corrosion resistance of a newly developed La-based bulk metallic glass with poor corrosion resistance. It is found that the alloys after ion implantation with doses ranging 6×10^{16}–1×10^{17} Nb/cm^2 have a remarkable enhancement of corrosion resistance in chloride containing environments and acid solution with respect to the alloy without the surface treatment while the implanted alloys still have high glass forming ability. The improvement of corrosion resistance for the implanted alloys is attributed to the high passivating ability of the Nb-containing surface layer. These results obtained here clearly demonstrate that the ion-implantation technique could be a useful method to improve the corrosion resistance of bulk metallic glasses without losing glass forming ability of alloys.

Keywords: A. Composites; B. Glasses, metallic; B. Corrosion; C. Casting

1. Introduction

In the last 14 years, many multi-component bulk metallic glass (BMG) systems with a critical cooling rate less than 100 K/s for glass formation and a size larger than 10 mm have been discovered using conventional copper mould casting, such as Zr- [1–3], Pd- [4,5], Mg- [6], Cu- [7,8], Fe- [9–11], Ca- [12], Y- [13] and rare earth (RE)-based [14–19] BMGs. Among them, only Pd-, Zr-, Y-, Mg- and La-based systems can form BMGs with critical sizes larger than 20 mm, which are desirable for their industrial applications. In general, BMGs, due to free defects associated with crystalline state such as grain boundaries, dislocations and stacking faults, are regarded as materials with high corrosion resistance. However, Mg- and La-based BMGs exhibit poor corrosion resistance. One common method applied to improve corrosion resistance of BMGs is alloying with specific elements, e.g., Nb and Ta, which will, consequently, reduce the glass forming ability of a given system [20]. Therefore, development of other methods, which can achieve both enhancement of corrosion resistance and no deterioration of glass forming ability, is strongly demanded in the BMG research field. In this paper, an ion-implantation technique was applied to improve corrosion resistance of a La-based BMG, as a prototype. The results obtained here clearly demonstrate that this technique could be a useful method to reach both criteria: enhancement of corrosion

* Corresponding author. Tel./fax: +86 571 8795 2107.
** Corresponding author.
E-mail addresses: clqin@imr.tohoku.ac.jp (C.L. Qin), jiangjz@zju.edu.cn (J.Z. Jiang).

0966-9795/$ - see front matter © 2007 Elsevier Ltd. All rights reserved.
doi:10.1016/j.intermet.2007.09.009

resistance and keeping high glass forming ability of bulk metallic glasses.

2. Experimental

Master ingots with nominal compositions of $La_{62}Al_{14}Cu_{11.7}Ag_{2.3}Ni_5Co_5$ were directly arc melted in Ti-gettered high-purity argon atmosphere. The purities of the elements are ranging from 99.5 at.% to 99.98 at.%. The ingots were remelted at least four times to achieve chemical homogeneity. For all tested experiments, rod samples (with a diameter of 5 mm) were prepared by suction-casting in copper molds under a purified argon atmosphere. The sample surfaces were mechanically polished and then implanted by niobium ions accelerated with 30 kV in various doses of 1×10^{16} ions/cm^2, 3×10^{16} ions/cm^2, 6×10^{16} ions/cm^2 and 1×10^{17} ions/cm^2 using an MEVVA (Metal Vapor Vacuum Arc) ion implantor at room temperature. The flux of the niobium ions was about 0.5 mA. The concentration depth profiles of implanted Nb atoms in the near surface layer were determined by the Rutherford Backscattering Spectroscopy (RBS) technique. The RBS experiments were performed in a scattering vacuum chamber, using 2 MeV He^+ generated from a tandem accelerator at IMR, Tohoku University. The amorphous nature of as-cast and implanted samples was verified by using a Thermo ARL X'Tra diffractometer with Cu K_α radiation at 45 kV. Vickers hardness of as-prepared samples was measured under 200 g load by a Vickers diamond pyramidal microhardness tester (MH5, China) at room temperature. Corrosion behavior of all samples was evaluated by electrochemical measurements. Anodic polarization curves were measured with a potential sweep rate of 50 mV min^{-1} after open-circuit immersion for about 10 min when the open-circuit potential became almost steady. A platinum mesh and a Ag/AgCl electrode were used as counter and reference electrodes, respectively. Surface morphologies of samples before and after electrochemical measurements were examined by field emission scanning electron microscope (FESEM, SIRION-100).

3. Results and discussion

Fig. 1a shows the XRD patterns of the as-cast $La_{62}Al_{14}Cu_{11.7}Ag_{2.3}Ni_5Co_5$ and implanted samples with various Nb doses. No obvious crystalline peaks were detected in all samples, indicating their fully amorphous nature even after ion-implantation treatments. This reveals that the thermal effect and alloying by ion implantation do not induce crystallization of the La-based BMG. Fig. 1b shows the depth profiles of implanted Nb for three implanted samples. Depth profiles of Nb atoms were evaluated using a surface energy approximation and the Bragg rule [21]. It reveals that the concentration of Nb atoms distributes along depth in the range of 0–100 nm. The maximum concentration of Nb atoms shifts from 55 nm for 3×10^{16} Nb/cm^2, 40 nm for 6×10^{16} Nb/cm^2, to 30 nm for 1×10^{17} Nb/cm^2. Two different spots on the same 1×10^{17} Nb/cm^2 implanted sample surface (not shown here) show almost the same depth profile, indicating that the implantation was performed quite uniformly in the area, and the reproducibility was very good. The concentration depth profile roughly corresponds to the projected range distribution of the incident Nb ions at the beginning of the implantation. With increasing the incident Nb influence, the profile moved to the surface, but the Nb atoms did not diffuse into the interior of the sample. Although the Nb content in the implanted layer is relatively high, the implanted layer still remains amorphous. Vickers hardness was found almost the same within experimental uncertainty, to be 191 ± 3, 194 ± 3, 191 ± 3, 192 ± 3 and 190 ± 3 for as-cast alloy and implanted samples for 1×10^{16} Nb/cm^2, 3×10^{16} Nb/cm^2, 6×10^{16} Nb/cm^2 and 1×10^{17} Nb/cm^2, respectively.

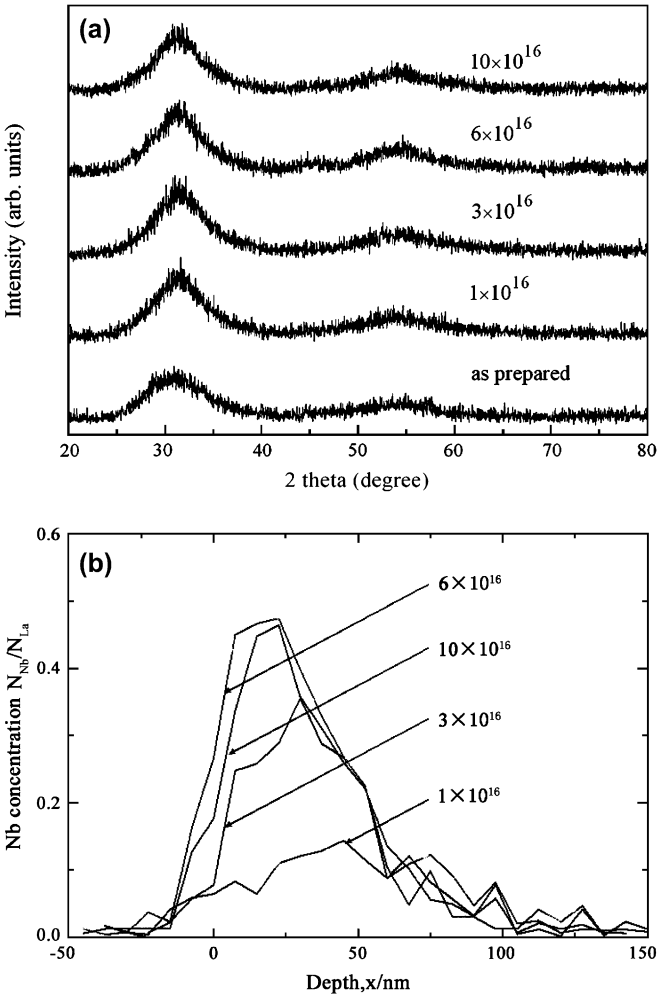

Fig. 1. (a) XRD patterns of the as-cast $La_{62}Al_{14}Cu_{11.7}Ag_{2.3}Ni_5Co_5$ and implanted samples with various Nb doses and (b) Nb concentration as a function of depth for implanted $La_{62}Al_{14}Cu_{11.7}Ag_{2.3}Ni_5Co_5$ bulk metallic glasses with various Nb doses. For the 1×10^{17} Nb/cm^2 implanted sample, two different spots (or areas) on the same surface were measured.

Fig. 2 shows the anodic polarization curves of the as-cast La-based BMG rods with and without surface treatments in 0.01 N NaCl and pH 2 H_2SO_4 solutions, respectively, open to air at 298 K. In 0.01 N NaCl (Fig. 2a), the as-cast $La_{62}Al_{14}Cu_{11.7}Ag_{2.3}Ni_5Co_5$ (marked as Nb0) and implanted samples with 1×10^{16} Nb/cm^2 (marked as Nb1) alloys dissolve

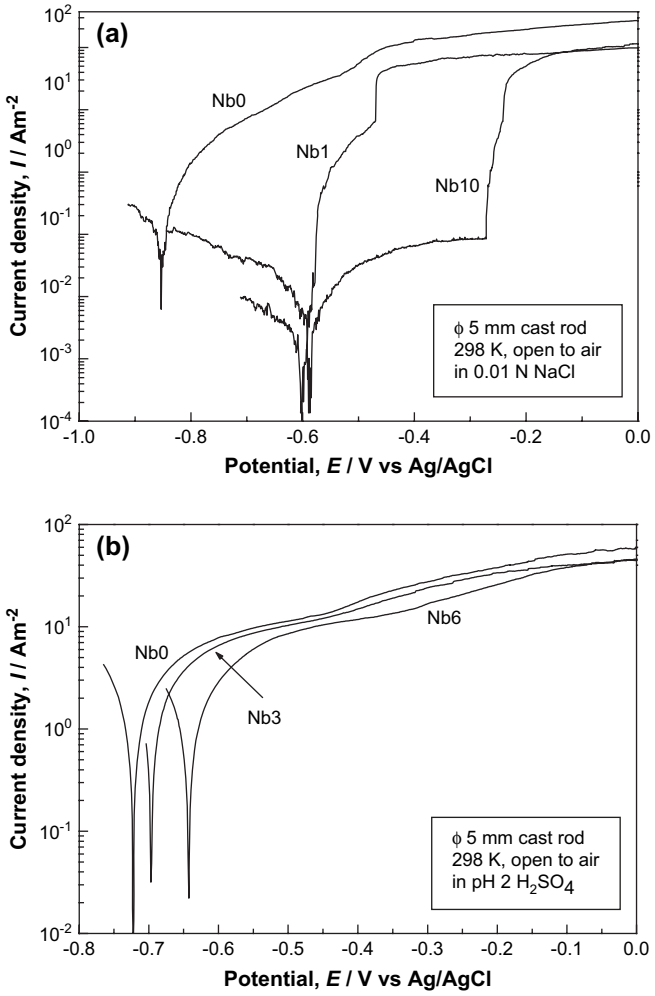

Fig. 2. (a) Anodic polarization curves of the as-cast $La_{62}Al_{14}Cu_{11.7}Ag_{2.3}Ni_5Co_5$ (marked as Nb0) and implanted samples with 1×10^{16} Nb/cm^2 (marked as Nb1) and 1×10^{17} Nb/cm^2 (marked as Nb10) Nb doses in 0.01 N NaCl solution at 298 K open to air. (b) Anodic polarization curves of the as-cast $La_{62}Al_{14}Cu_{11.7}Ag_{2.3}Ni_5Co_5$ (marked as Nb0) and implanted samples with 3×10^{16} Nb/cm^2 (marked as Nb3) and 6×10^{16} Nb/cm^2 (marked as Nb6) Nb doses in H_2SO_4 solution with pH = 2 at 298 K open to air.

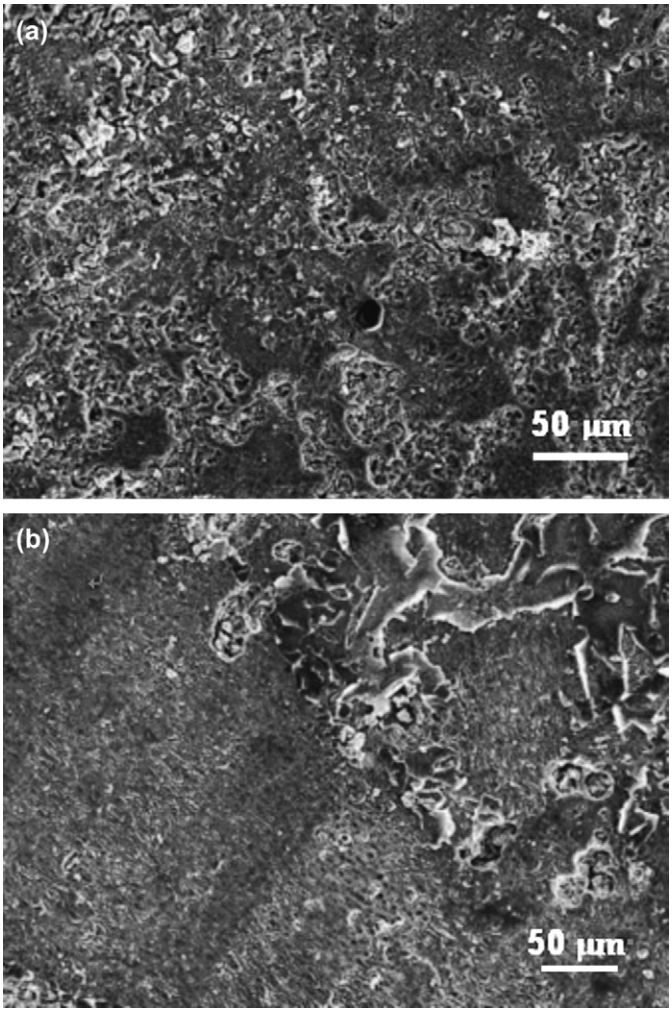

Fig. 3. SEM images for implanted $La_{62}Al_{14}Cu_{11.7}Ag_{2.3}Ni_5Co_5$ samples after polarization measurements in 0.01 N NaCl solution at 298 K open to air (Fig. 2a); (a) and (b) are for implanted samples with 1×10^{16} Nb/cm^2 and 1×10^{17} Nb/cm^2 doses, respectively.

actively and their anodic current densities increase quickly by anodic polarization. It is found that the corrosion potential shifts to higher values when the surface of the alloy is treated by ion implantation. The significant improvement in corrosion resistance is observed for the implanted alloy with 1×10^{17} Nb/cm^2 (marked as Nb10). The Nb10 alloy is spontaneously passivated with a low anodic current density and a wide passive region (−0.5 V to −0.27 V), although it suffers pitting. Pit nucleation appears at potentials of −0.52 V, −0.47 V and −0.27 V versus Ag/AgCl for the Nb0, Nb1 and Nb10 alloys, respectively. (Note that the value of the pitting potential for the Nb0 alloy is roughly estimated.) The formation of pits was further confirmed by SEM observation after anodic polarization as shown in Fig. 3. The Nb10 alloy shows nobler pitting potential and lower anodic current density, leading to the reduction of pitting susceptibility and the improvement of pitting corrosion resistance. Accordingly, ion-implantation technique is effective for modifying the surface and enhancing the pitting corrosion potential against localized corrosion in chloride containing environments. In pH 2 H_2SO_4 solution (Fig. 2b), alloys exhibit similar anodic polarization behavior. Their anodic polarization curves are characterized by an active region in which the current density increases rapidly over a narrow potential range, followed by a slow rate of increase with increasing potential. However, the implantation of Nb element to the alloy surface causes the ennoblement of the corrosion potential from −0.72 V for the as-cast alloy (Nb0), −0.70 V for the 3×10^{16} Nb/cm^2 implanted alloy (Nb3) to −0.64 V for the 6×10^{16} Nb/cm^2 implanted alloy (Nb6) and the decrease of anodic current density. These results clearly reveal that corrosion resistance in acid solution is improved for the Nb-implanted BMG alloys.

After anodic polarization in NaCl and H_2SO_4 solutions, the surfaces of the Nb1 (Fig. 3a), Nb10 (Fig. 3b), Nb3 (Fig. 4a and b) and Nb6 (Fig. 4c) alloys were further examined by SEM. The image in Fig. 3a shows serious corrosion attack

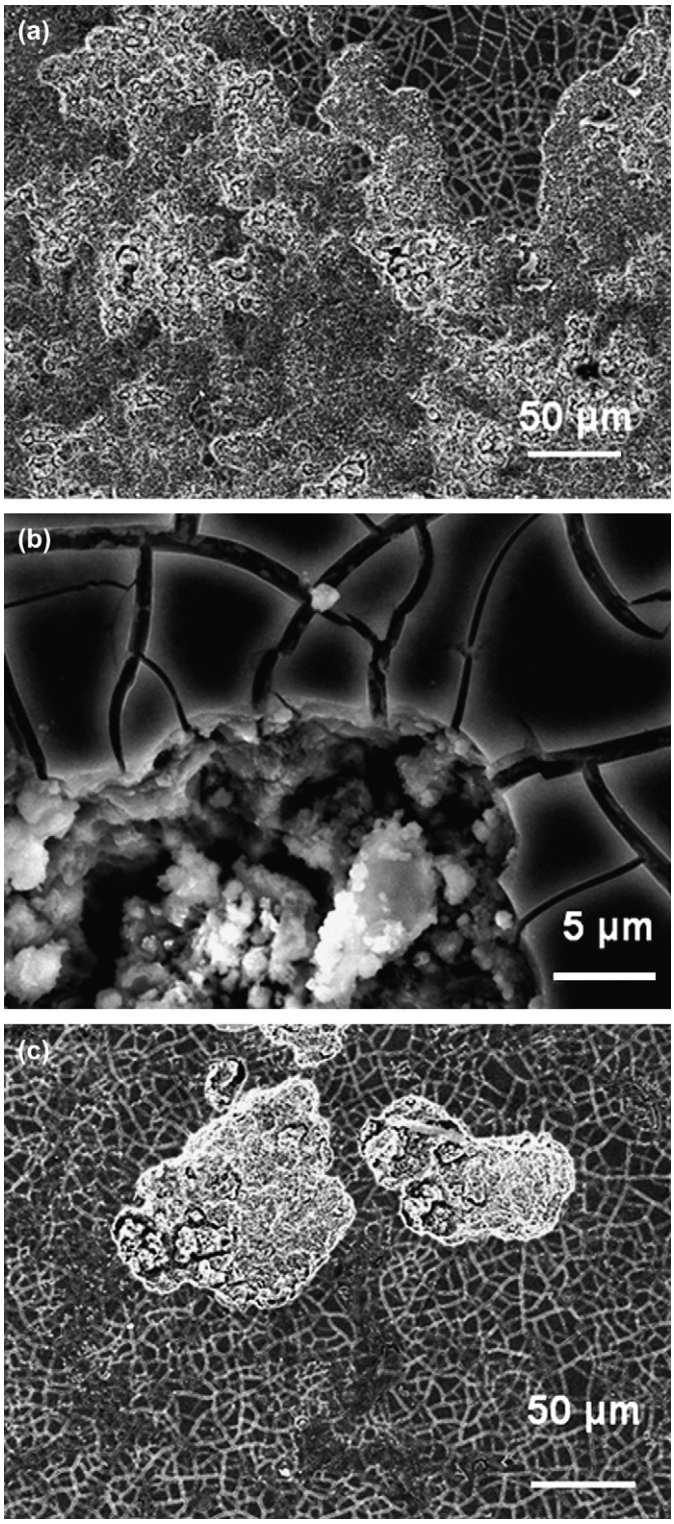

Fig. 4. SEM images for implanted $La_{62}Al_{14}Cu_{11.7}Ag_{2.3}Ni_5Co_5$ samples after polarization measurements in H_2SO_4 solution with pH = 2 at 298 K open to air (Fig. 2b); (a), (b) and (c) are for implanted samples with 3×10^{16} Nb/cm^2, 3×10^{16} Nb/cm^2 and 6×10^{16} Nb/cm^2 doses, respectively.

on the surface after anodic polarization. Corrosive products and cracks can be detected throughout the entire sample surface. In contrast, the image in Fig. 3b consists of two different regions, i.e., a relatively flat region and peel-like region. Several of pits can also be detected in the image. EDX analyses show that Nb concentration is about eight times larger in the peel-like region than that in the flat region. It seems that the corrosion initially attacks the outer surface and further corrodes the substrate after the Nb-containing surface layer is cracked, pitted and peeled off. Larger flat areas (of substrate surface) are observed for the Nb10 alloy after anodic polarization in Fig. 3b, as compared with those for the Nb1 alloy. This indicates that a certain amount of Nb concentration in the surface layer is required to reach a large enhancement of corrosion resistance of the alloy, which is in agreement with the results obtained in Fig. 2a. The 3×10^{16} Nb/cm^2 implanted alloy with relatively low Nb concentration in the surface layer still suffers severe corrosion in pH = 2 H_2SO_4 solution, as shown in Fig. 4a. During the polarization process, pits initiate, develop and joint together to form corrosive products covering a large fraction of alloy surface, accompanied by active dissolution of the alloy. High magnification image (Fig. 4b) gives evidence that a pit is formed in the flat region containing high-density cracks. After polarization, the surface of the 6×10^{16} Nb/cm^2 implanted alloy in Fig. 4c has much less pitting regions as compared to the Nb3 alloy, mainly consisting in a flat region containing high-density cracks. The cracks observed in Fig. 4 might be caused by hydrogen, which was formed during polarization measurements. To understand the formation process of cracks during polarization measurements, more studies are required. These results obtained in Figs. 2b and 4 also suggest that the Nb-implanted La-based BMG alloys have relatively higher corrosion resistance in pH = 2 H_2SO_4 solution as compared to as-cast BMG alloy.

4. Summary

In conclusion, the ion-implantation technique has been applied to improve the corrosion resistance of the newly developed $La_{62}Al_{14}Cu_{11.7}Ag_{2.3}Ni_5Co_5$ BMG having poor corrosion resistance. It is found that the alloys after ion implantation with doses ranging 6×10^{16}–1×10^{17} Nb/cm^2 have a remarkable enhancement of corrosion resistance in chloride containing environments and acid solution with respect to the alloy without the surface treatment while the implanted alloys still have high glass forming ability. The improvement of corrosion resistance of the alloy is attributed to the high passivating ability of the Nb-containing surface layer (about 100 nm). By further optimizing element type, dose, energy, substance temperature, thickness and homogeneity of implanted surface layer, higher corrosion resistance of the La-based BMG could be expected. These results obtained here clearly demonstrate that the ion-implantation technique could be a useful method to improve the corrosion resistance of bulk metallic glasses without losing glass forming ability of alloys.

Acknowledgments

The authors would like to thank HASYLAB in Germany, BSRF in Beijing, NSRL in Hefei, KEK in Japan, and APS in

USA for use of the synchrotron radiation facilities. Financial support from the National Natural Science Foundation of China (Grants No. 50341032, 50425102, 50601021, 5070138 and 60776014), Zhejiang University–Helmholtz Cooperation fund, the Ministry of Education of China (Program for Changjiang Scholars), Y.C. Tang Disciplinary Development Fund, Zhejiang University is gratefully acknowledged.

References

[1] Peker A, Johnson WL. Appl Phys Lett 1993;63:2342.
[2] Inoue A, Yokoyama Y, Shinohara Y, Masumoto T. Mater Trans JIM 1994;35:923.
[3] Zhang GQ, Jiang QK, Chen LY, Shao M, Liu JF, Jiang JZ. J Alloys Compd 2006;242:176.
[4] Inoue A, Zhang T, Nishiyama N, Ohba K, Masumoto T. Mater Trans JIM 1993;34:1234.
[5] He Y, Schwarz RB, Archuleta JI. Appl Phys Lett 1996;69:1861.
[6] Ma H, Shi LL, Xu J, Li Y, Ma E. Appl Phys Lett 2005;87:181915.
[7] Xu DH, Duan G, Johnson WL. Phys Rev Lett 2004;92:245504.
[8] Dai CL, Hua G, Yong S, Li Y, Ma E, Xu J. Scr Mater 2006;54:1403.
[9] Lu ZP, Liu CT, Thompson JR, Porter WD. Phys Rev Lett 2004;92:245503.
[10] Ponnambalam V, Poon SJ, Shiflet GJ. J Mater Res 2004;19:1320.
[11] Shen J, Chen QJ, Sun JF, Fan HB, Wang G. Appl Phys Lett 2005;86:151907.
[12] Park ES, Kim DH. Appl Phys Lett 2005;86:201912.
[13] Guo FQ, Poon SJ, Shiflet GJ. Appl Phys Lett 2005;83:2575.
[14] Zhang Y, Tan H, Li Y. Mater Sci Eng A 2004;436:375.
[15] Li R, Pang SJ, Men H, Ma CL, Zhang T. Scr Mater 2006;54:1123.
[16] Zhang B, Wang RJ, Zhao DQ, Pan MX, Wang WH. Phys Rev B 2006;73:092201.
[17] Jiang QK, Zhang GQ, Chen LY, Wu JZ, Zhang HG, Jiang JZ. J Alloys Compd 2006;424:183.
[18] Jiang QK, Zhang GQ, Chen LY, Jiang JZ. J Alloys Compd 2006;424:179.
[19] Jiang QK, Zhang GQ, Yang L, Wang XD, Saksl K, Franz H, et al. Acta Mater 2007;55:4409.
[20] Qin CL, Asami K, Zhang T, Zhang W, Inoue A. Mater Trans 2003;44:749.
[21] Tesmer JR, Nastasi M, editors. Handbook of modern ion beam materials analysis. Pittsburgh: Materials Research Society; 1995. p. 37–81.